ELSEVIER

Chemical Geology 237 (2007) 384–400

CHEMICAL GEOLOGY
INCLUDING
ISOTOPE GEOSCIENCE

www.elsevier.com/locate/chemgeo

Chloride and carbonate immiscible liquids at the closure of the kimberlite magma evolution (Udachnaya-East kimberlite, Siberia)

Vadim S. Kamenetsky [a,*], Maya B. Kamenetsky [a], Victor V. Sharygin [b], Kevin Faure [c], Alexander V. Golovin [b]

[a] *Centre for Ore Deposit Research and School of Earth Sciences, University of Tasmania, Hobart, Tasmania 7001, Australia*
[b] *Institute of Geology and Mineralogy, Siberian Branch of Russian Academy of Sciences, Novosibirsk, Russia*
[c] *Institute of Geological and Nuclear Sciences, PO Box 31-312, Lower Hutt, New Zealand*

Accepted 15 July 2006

Editor: R.L. Rudnick

Abstract

The compositions of parental magmas forming kimberlitic rocks remain largely unknown because of masking effects of syn-eruptive contamination and degassing, and post-magmatic alteration. Among most affected elements are volatiles (H_2O and CO_2) and alkalies (Na and K). This study attempts to overcome the problems related to the alteration of kimberlites by detailed petrographic and chemical analyses of exceptionally fresh, and thus essentially anhydrous (<0.5 wt.% H_2O), kimberlite samples from the Udachnaya-East pipe (Daldyn–Alakit region, Siberia). The groundmass of these kimberlites contains abundant carbonate (calcite, shortite, zemkorite) and chloride (halite, sylvite) minerals, cementing olivine phenocrysts, and forming round segregations ("nodules"). The nodules, belonging to the chloride and chloride–carbonate types, show no evidence of thermometamorphic effects on the contacts with the host kimberlite. The chloride–carbonate nodules demonstrate liquid immiscibility textures that are remarkably similar to those observed in the olivine-hosted chloride–carbonate melt inclusions at ~600 °C. The similarity of oxygen and carbon isotope values of carbonates from the groundmass and nodules ($\delta^{18}O$ 12.5 to 13.9‰ VSMOW; $\delta^{13}C$ –3.7 to –2.7‰ VPDB) points to their common origin at similar temperatures. We argue for crystallisation of the chloride–carbonate nodules from residual kimberlite melts, pooled after exhaustion of the silicate melt component. The enrichment of the residual melt in alkali carbonate and chloride is partly reflected in the bulk groundmass compositions (10–11 wt.% CO_2, 2.3–3.2 wt.% Cl, 2.6–3.7 wt.% Na, and 1.6–2.0 wt.% K). We propose that this enrichment is inherited from the kimberlite parental magma, and it can be responsible for the kimberlite low liquidus temperatures, low viscosities, and rapid emplacement.

Keywords: Kimberlite; Immiscibility; Chloride; Carbonate; Melt inclusions; Carbon and oxygen isotopes

1. Introduction

Kimberlite magmas are in many aspects unusual compared to other terrestrial magmatic liquids. They are renowned for carrying diamonds, but the kimberlite-diamond genetic links are still elusive. Despite significant research efforts, there is still uncertainty about the

* Corresponding author. Tel.: +61 362267649; fax: +61 362232547.
E-mail address: Dima.Kamenetsky@utas.edu.au (V.S. Kamenetsky).

0009-2541/$ - see front matter © 2006 Elsevier B.V. All rights reserved.
doi:10.1016/j.chemgeo.2006.07.010

true chemical identity of kimberlite parental melts and their derivates. Kimberlite magmas are often contaminated by large quantities of lithic fragments and crystals, unrelated to the evolution of the parental melt. In most cases kimberlites are severely modified by syn- and post-magmatic changes that have altered the original alkali and volatile element abundances. These problems are reflected in the definition of the kimberlite rock as "*both a contaminated and altered sample of its parent melt*" (Pasteris, 1984). Numerous other definitions of the kimberlite commonly reflect on ultramafic compositions and enrichment in volatiles (CO_2 and H_2O) (Skinner and Clement, 1979; Clement et al., 1984; Mitchell, 1986) which are supposedly inherited from parental magmas.

The ultramafic silicate compositions of kimberlites are ascribed to abundant olivine phenocrysts (olivine-II) in the groundmass, whereas significant CO_2 and H_2O abundances are attributed respectively to carbonate minerals (calcite and dolomite) and serpentine (+ other H_2O-bearing magnesian silicates). It is still debatable whether all measured H_2O in kimberlites had magmatic origin or was partly introduced post-emplacement (Sheppard and Dawson, 1975). On the other hand, shallow-level evolution of the volatile-rich kimberlite melt can be accompanied by the loss of volatiles (particularly CO_2). This is another factor complicating quantification of the parental melt composition if inferred from bulk kimberlite analyses.

In general, the broad compositional range of kimberlites is defined by two end-members, magnesian silicate (olivine and serpentine) and carbonatitic (calcite). Thus, the kimberlites worldwide form a trend between these two end-members, Mg-rich and Ca-rich

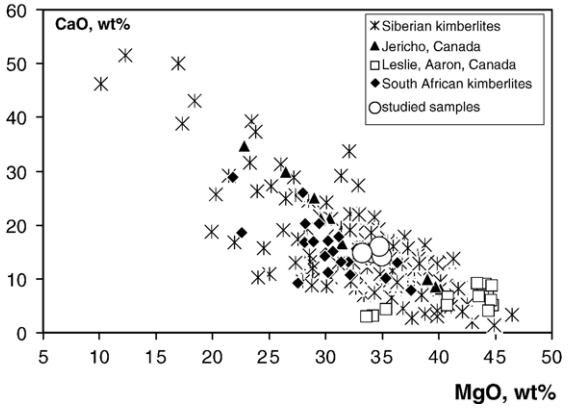

Fig. 1. MgO vs CaO compositional co-variations among Group I kimberlites from Siberia, South Africa and Canada (Price et al., 2000; Vasilenko et al., 2002; Bogatikov et al., 2004; Fedortchouk and Canil, 2004; Harris et al., 2004; Becker and le Roex, 2006). All compositions are recalculated to 100 wt.% on a volatile-free basis.

respectively (Fig. 1). It is likely that several processes can account for this compositional array. For example, crystallisation of olivine and segregation of carbonatitic melt (Ca increase) is counter-balanced by olivine accumulation and removal of carbonatitic melt (Ca decrease). Whatever the reason for the build-up in Ca, a general consensus exists that the magmatic carbonatitic component is an integral part of all kimberlite rocks, and their parental magmas. What still remains to be understood is why an expected increase in concentrations of alkali elements (Na and K) during the evolution of the kimberlite magmas is not reflected in the compositions of common kimberlites (e.g., Na_2O is invariably <0.3 wt.%). Moreover, low abundances of these elements relative to the elements of similar incompatibility are not easily reconciled with expected geochemical characteristics of low-degree mantle melts, even if residual phlogopite is present in the source peridotite (le Roex et al., 2003).

The idea of an alkali element loss and an H_2O gain in kimberlites during post-magmatic processes can be promoted based on the fact that all kimberlites studied to date are, to some extent, altered rocks. The alteration of the carbonate fraction towards essentially alkali-free calcitic compositions has been advocated since the discovery of modern alkali natrocarbonatite lavas from the Oldoinyo Lengai volcano and their altered counterparts (Dawson, 1962; Gittins and McKie, 1980; Hay, 1983; Deans and Roberts, 1984; Clarke and Roberts, 1986; Dawson et al., 1987; Dawson, 1989). Rapid degradation of alkali carbonates and dissolution of alkali chlorides in crustal environments can be responsible for depriving kimberlites (carbonatites) of their original sodium and potassium. But how do we learn about magmatic alkali abundances in kimberlites without having an "Oldoinyo Lengai" case among kimberlites?

This paper provides unequivocal evidence for the preservation of alkali carbonates and chlorides in the groundmass and olivine-hosted melt inclusions in at least some kimberlitic rocks. Our example of an unaltered kimberlite of the diamondiferous Udachnaya-East pipe in Siberia reveals the presence of significant quantities of non-silicate melt components in a common Group I kimberlite magma. We propose that an essentially non-silicate melt aggregated within the solidifying kimberlite groundmass and underwent carbonate–chloride unmixing at temperatures <600 °C.

2. Udachnaya-East kimberlite: location and samples

The Udachnaya diamondiferous kimberlite pipe is located in the Daldyn–Alakit region of the Siberian

diamondiferous kimberlite province. Most Siberian pipes are tuff-breccias essentially devoid of unaltered olivine, but some contain large blocks of massive fresh kimberlite. A remarkable characteristic of this region is that it contains more pipes with fresh, unaltered olivine than any other kimberlite region within the Siberian province. About 10% of the intrusions exhibit either two adjacent channelways or repeated intrusion of magma through the same chimney. The Udachnaya pipe, the best known example of these twin diatremes, is located in the northwest part of the Daldyn field. At the surface it consists of two adjacent bodies (East and West) that are separated at depth >250–270 m. Based on stratigraphic relationships both intrusions formed at the Devonian–Carboniferous boundary (~350 Ma), and the age estimates vary from 389 to 335 Ma (Maslovskaja et al., 1983; Burgess et al., 1992; Kinny et al., 1997; Maas et al., 2005). The eastern and western bodies of the Udachnaya kimberlite pipe are different from each other in terms of mineralogy, petrography, composition, and degree of alteration. As the alteration of the western pipe can be considered as typical of this rock type, the rocks of the Udachnaya-East are unique in having lesser alteration, and in some places they are completely unaltered.

At depths greater than 350 m a particularly fresh kimberlite has been found in the Udachnaya-East pipe. These rocks are described as dark-grey massive kimberlite, characterized by unaltered euhedral–subhedral olivine phenocrysts set in a dominantly carbonate matrix (Marshintsev et al., 1976; Marshintsev, 1986). A considerably lower amount of xenolithic material occurs here compared to the upper part of the pipe (Marshintsev et al., 1976). At deeper levels (>400 m) of the kimberlite body the amount of serpentine in the groundmass gradually decreases and the amount of carbonate in the groundmass increases. The origin of carbonate (i.e., primary vs secondary) is still a matter of considerable debate in the Russian literature (Marshintsev et al., 1976; Mal'kov and Bobolovich, 1977; Marshintsev, 1986; Ukhanov et al., 1988; Zinchuk et al., 1993). Intensive mining of the Udachnaya pipe revealed widespread chloride minerals (mostly halite) as dispersed masses in the groundmass and massive multi-mineral segregations of halite, serpentine, anhydrite, carbonates and hydrous iron oxides (Pavlov and Ilupin, 1973). The amount of chloride minerals in the groundmass increases with depth, and recently a large number of chloride–carbonate "nodules" were recovered from ~470–500 m depths of the mine.

Kimberlites in our study are dark massive rocks with porphyroclastic fragmental textures. A fine- to coarse-grained groundmass comprises a mixture of euhedral olivine, phlogopite, perovskite, zoned spinel (Cr-spinel–titanomagnetite–magnetite), calcite, Na–K–Ca carbonates, Na–K chlorides, pyrrhotite and K-sulphides (Sobolev et al., 1989; Golovin et al., 2003; Sharygin et al., 2003; Kamenetsky et al., 2004). Monticellite, sodalite, rutile, ilmenite, and sulphates occur occasionally. Some varieties of the kimberlite are characterised by higher amounts of monticellite and sodalite in small veins and segregations. Groundmass olivine, the main phenocrystic mineral of the kimberlitic melt, is very abundant (up to 40–50 vol.%), completely unaltered, and represented by relatively small (0.2–0.8 mm) euhedral, colourless or slightly greenish, flattened grains. Almost all groundmass olivine crystals have cores with highly variable Fo contents (85.5–93.5 mol%) and very homogeneous (89.0±0.2 mol%) rim zones. Olivine contains abundant crystal, fluid and melt inclusions (Golovin et al., 2003; Kamenetsky et al., 2004).

The compositions of kimberlite groundmass (hand picked from olivine macrocrysts and fragments of country rocks) are characterised by typical kimberlite silica undersaturation (25.2–27.1 wt.% SiO_2) and low Al_2O_3 (1.74–2.13 wt.%), but high CaO (12.04–12.70) wt.% and CO_2 (9.83–10.71 wt.%) contents (Table 1). Trace element compositions are similar to those of other kimberlites, having incompatible element enrichment and depletion in heavy rare-earth elements and Y. The radiogenic isotope data ($^{87}Sr/^{86}Sr_t \approx 0.7047$, $\varepsilon_{Nd} \approx +4$, $^{206}Pb/^{204}Pb_t \approx 18.7$, $^{207}Pb/^{204}Pb_t = 15.53$, $^{208}Pb/^{204}Pb_t = 35.5–38.9$, t=367 Ma; Maas et al., 2005) fall within the field defined by most group-I kimberlites (Smith, 1983; Fraser et al., 1985; Weis and Demaiffe, 1985). The overall petrographic, mineralogical and chemical characteristics of the Udachnaya-East kimberlites suggest that they are common type-I (Mitchell, 1989) or group-I (Smith, 1983; Smith et al., 1985) kimberlite. However, the studied three samples are distinctly different from other kimberlites in that they have high abundances of alkali elements (4.3–5.7 wt.% Na+K), strong enrichment in chlorine (2.3–3.2 wt.%), and extraordinary depletion in H_2O (<0.5 wt.%) coupled with absence of primary or secondary serpentine (Kamenetsky et al., 2004; Maas et al., 2005).

3. Chloride–carbonate nodules in kimberlite

The chloride–carbonate samples ("nodules") were collected from fresh kimberlite at the stockpiles of the Udachnaya-East pipe. The assumed depth of their origin in the mine pit is ~500 m. The nodules vary in size from a few cm to 0.5×1.5 m, but are commonly 5 to 30 cm across. The shapes are usually round and ellipsoidal, but angular nodules were also encountered. The nodules have very

Table 1
Compositions of host kimberlites, a chloride–carbonate nodule and its mineral constituents (in wt.%)

	1	2	3	4	5(16)	6(3)	7(13)	8(12)	9(2)	10(18)	11(7)
SiO_2	27.06	26.08	25.24	1.32	0	0	0	0	0	0	0
TiO_2	1.23	1.12	1.40	0.05	n.d.	n.d.	n.d.	n.d.	n.d.	n.d.	n.d.
Al_2O_3	2.13	1.74	2.11	0.09	n.d.	n.d.	n.d.	n.d.	n.d.	n.d.	n.d.
FeO_t	7.63	7.16	6.92	0.37	0.02	0.04	0.01	0.02	0	0.02	0.01
MgO	29.41	29.59	27.79	2.47	0	0	0	0	0	15.83	0.03
CaO	12.70	12.04	12.41	31.90	36.57	38.87	30.41	34.35	32.20	0.25	0.07
Na_2O	3.55	4.24	4.96	18.87	19.46	19.48	20.38	20.94	21.08	36.91	10.33
K_2O	1.97	2.33	2.39	2.41	0.10	0.26	6.88	6.17	3.59	0.62	41.24
P_2O_5	0.49	0.42	0.41	0.23	0.02	0.39	0.22	0.61	0.22	0.02	0.01
SO_3	0.55	0.67	0.82	1.45	0.02	0.09	6.70	2.04	3.25	0.06	48.31
Cl	2.28	3.05	3.20	4.32	0.01	0.10	0.06	0.09	0.57	14.26	0.01
SrO	0.11	0.10	0.11	0.25	0.35	0.63	0.58	0.59	0.58	0.04	0.01
BaO	0.13	0.13	0.14	0.05	0.06	0.10	0.14	0.14	0.09	0.08	0.04
CO_2	9.83	10.27	10.71	35.27	n.d.	n.d.	n.d.	n.d.	n.d.	n.d.	n.d.
H_2O	0.45	0.45	0.63	n.d.	n.d.	n.d.	n.d.	n.d.	n.d.	n.d.	n.d.
Total	99.52	99.39	99.24	99.05	56.61	59.96	65.38	64.95	61.58	68.09	100.06

(1–3) Groundmass of Udachnaya-East kimberlites (samples YBK-0, YBK-1 and YBK-3 respectively).
(4) Chloride–shortite–northupite nodule UV-2-03.
(5) Shortite (sample UV-2-03).
(6–9) Carbonate sheet along profile line (sample UV-5a-03, Fig. 4, from left to right).
(10) Northupite (sample UV-2-03).
(11) Aphthitalite segregations fringing carbonate sheets (Fig. 3D).
Numbers in brackets represent number of analytical spots;
FeOt — total Fe; n.d. — not determined.
Analyses of rocks and minerals were respectively performed by X-ray fluorescence (Phillips 1400, University of Tasmania) and electron-microprobes (Cameca SX100, University of Tasmania and Camebax microbeam, IGM, Novosibirsk; analytical conditions: beam size — 10 μm, accelerating voltage — 20 kV; current — 10–12 nA). Chlorine in the rocks was analysed by ion chromatography (Analytical Services of Tasmania) using standard methods for the examination of water and wastewater proposed by the American Public Health Association (APHA methods). Carbon and hydrogen were determined by an elemental analyser Carlo Erba CHNS-O (University of Tasmania).

distinct contacts with the host kimberlite, but without any thermometamorphic effects. The contacts are composed of thin (<1 mm) breccia-like aggregate of olivine, calcite, sodalite, phlogopite–tetraferriphlogopite, humite–clinohumite, Fe–Mg carbonates, perovskite, apatite, magnetite, djerfisherite ($K_6(Cu,Fe,Ni)_{25}S_{26}Cl$) and alkali sulphates in a matrix of chlorides. Olivine grains present at the contact with nodules belong to two types: zoned euhedral crystals similar to the Udachnaya-East groundmass olivine-II, and grains with highly irregular shapes and "mosaic" distributions of Fe–Mg (Fig. 2D). Carbonate and sulphate grains are often present as "skeletal" crystals (Fig. 2E, F).

Based on mineralogy the nodules can be separated into two major groups — chloride and chloride–carbonate. Chloride minerals are mainly represented by halite with included round grains of sylvite, and rare sylvite grains with halite inclusions. The grain size, halite colour and transparency are highly variable, ranging from translucent to milky white and from white to all shades of blue. White and blue halite is often randomly interspersed, although in some coarse-grained nodules the interior parts are blue and dark-blue coloured, whereas rims are almost colourless. Chloride nodules always contain variable amount of fine-grained silicate–carbonate material (from 1 to 20 vol.%) that is either present interstitially among halite crystals or forms irregular compact masses veined by chlorides. Contacts between silicate–carbonate material and chlorides are decorated by euhedral grains of olivine, monticellite, djerfisherite, perovskite, pyrrhotite, shortite and magnetite.

Chloride–carbonate nodules contain roughly similar amounts of chloride and carbonate minerals that are regularly interspersed (Figs. 2A–C, 9B). Carbonates are present as 1–5 mm thick sheets with a bumpy or boudin-like surface. The groups of aligned, subparallel sheets make up rhombohedron formations (2–2.5 cm) that resemble hollow (skeletal) carbonate crystals (~78° angle) in shape. Cross-sections of inflated parts of the sheets show symmetrical zoning that reflects the change from translucent to milky-white carbonate (Figs. 2A, B, 9B). The intra-sheet space and cracks in carbonate sheets are filled with sugary aggregates of chloride minerals. A texturally and mineralogically different

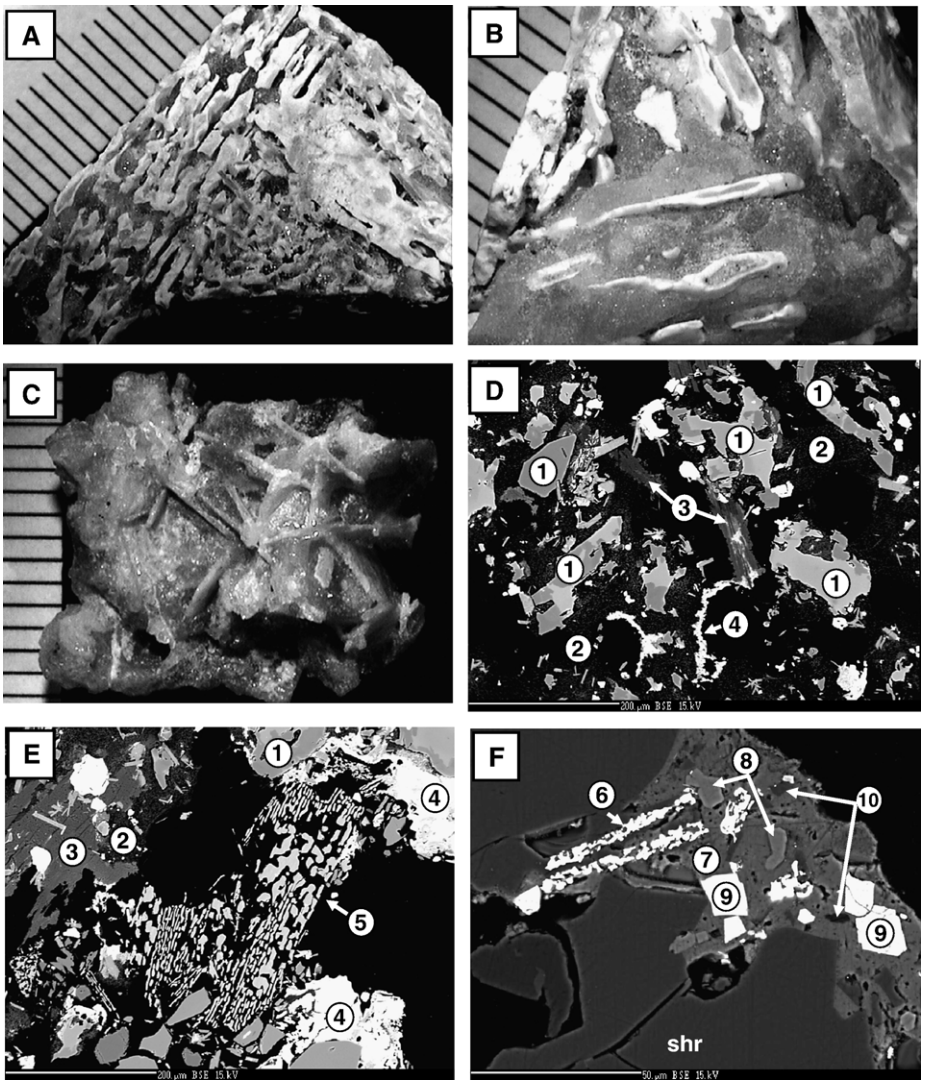

Fig. 2. Textural characteristics and mineral relationships in the chloride–carbonate nodules. A, B — sample UV-5a-03 show texture resembling liquid immiscibility; white zoned sheets are composed of carbonates (Na–Ca±K±S), greyish masses cementing sheets are chlorides (halite–sylvite). Scale: 1 graticule = 1 mm. C — sample UV-2-03, composed of shortite, northupite and chlorides. D–E — contact zones of nodule UV-2-03 and host kimberlite, composed of mozaic-structured olivine, chlorides, Mg-hydrosilicates and "skeletal" calcite (E). F — Skeletal Ba-sulphate and euhedral djerfisherite in a matrix cementing large shortite crystals (shr) in sample UV-2-03. 1— olivine; 2 — Mg-hydrosilicates (?); 3 — Mg carbonate (?); 4 — halite; 5 — calcite; 6 — Ba-sulphate; 7 — aphthitalite; 8 — apatite; 9 — djerfisherite; 10 — tetraferriphlogopite.

variety of the chloride–carbonate nodules is represented by a single sample UV-2-03 (Fig. 2C; Table 1). In this ~15 cm nodule, carbonates are present as very thin (<0.2 mm) aligned white calcite–shortite sheets, as well as individual well-formed yellowish crystals of shortite $Na_2Ca_2(CO_3)_3$ and northupite $Na_3Mg(CO_3)_2Cl$ (up to 1 cm). In the carbonate intergrowths northupite is interstitial and less abundant (25–30%), and can be distinguished from shortite by crystallographic properties and higher transparency.

4. Mineralogy of chloride–carbonate nodules

The chloride component of the nodules is dominated by halite, whereas individual grains of sylvite are rare. Typically, sylvite is included in halite, making up to 30 vol.% of the chloride assemblage, and in places halite is sprinkled with minute sylvite grains. Sometimes sylvite inclusions in halite show crystallographic outlines, however, round, lens-shaped and ameboid-like blebs of sylvite with different sizes and orientations are a

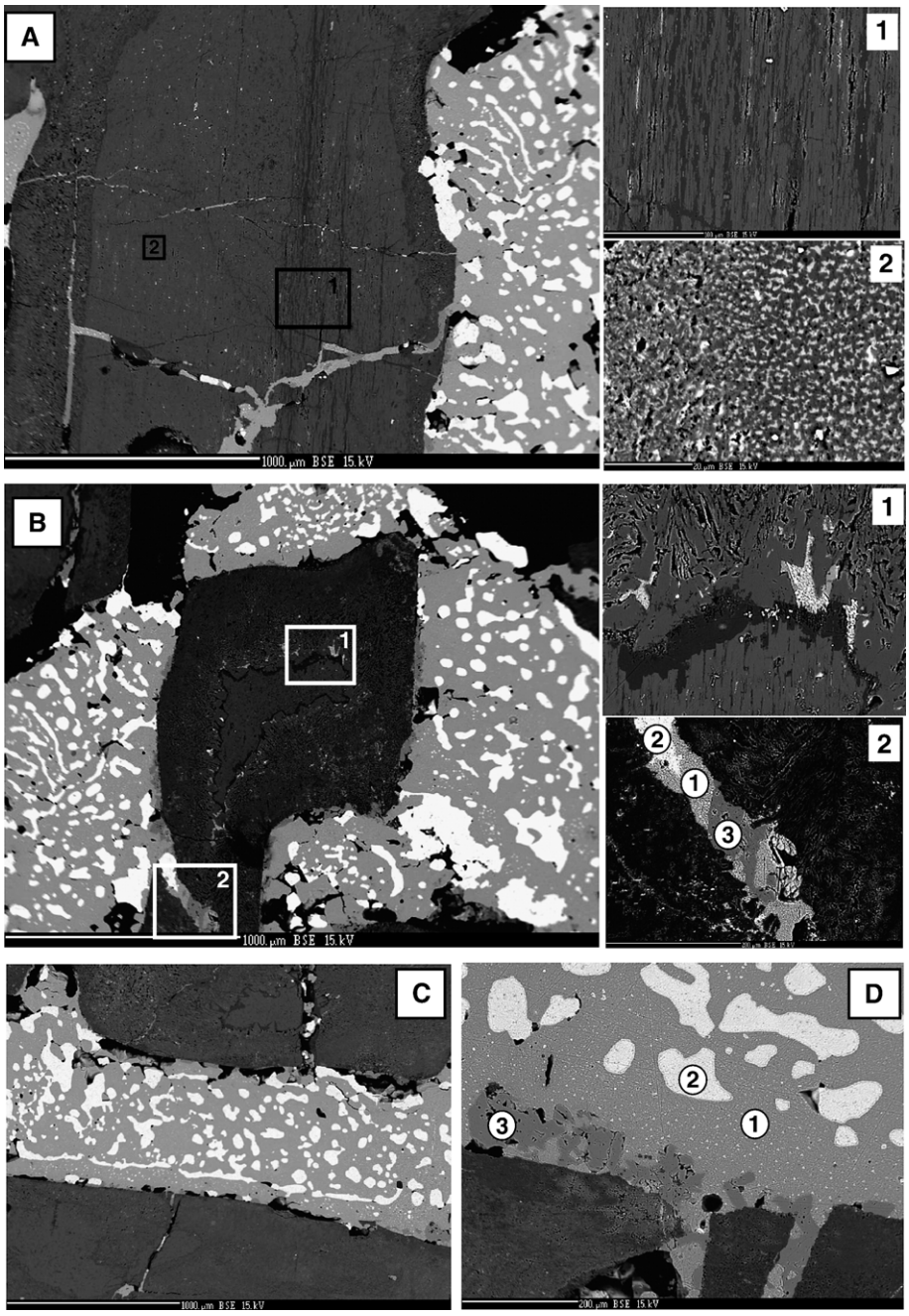

Fig. 3. Sample UV-5a-03. The nodule texture is determined by a carbonate–chloride grid. Chloride minerals are represented by massive halite, hosting amoeboid blebs of sylvite. Halite away from large sylvite formations is sprinkled with minute sylvite grains. Sometimes sylvite forms streaks that show distinctive alignment. The overall texture of chloride layers and shape and distribution of sylvite, are reminiscent of liquid immiscibility. Carbonate sheets are symmetrically zoned (A, B), and fine-scale heterogeneity is noted within zones (areas 1 on A and B). The outer carbonate zone is often porous. Irregular aphthitalite is present in halite, always near contacts with carbonate (D) and in veinlets in carbonate (B, area 2, D). Fine-grained aphthitalite is dispersed in inner parts of carbonate sheets (A, area 2). 1 — halite; 2 — sylvite; 3 — aphthitalite.

prominent feature of the chloride masses (Fig. 3). Sylvite domains are often extremely irregular in shape, with curved re-entrances and attenuated swellings. Some domains are thin and elongated, and they can be either subparallel or perpendicular to the contacts with the carbonate sheets (Fig. 3A–C). Although on polished surfaces sylvite shows round outlines, however, the overall texture is emulsion-like. The amoeboid shapes of

sylvite typically appear in three dimensions under examination in transparent light (Fig. 3). Chloride minerals also seal fractures cutting across the carbonate sheets and along the cleavage planes in carbonates (Fig. 3).

The carbonate sheets are very heterogeneous in texture and composition (Figs. 2A–C, 3, 4). In one case associated shortite, northupite and calcite were found (sample UV-2-03, Fig. 2C), whereas in other samples (UV-1-03 and UV-5a-03, Fig. 2A, B) the dominantly Na–Ca carbonates show zoning with respect to K_2O (decreasing from centre to rims). In some occurrences a patchy distribution of textures and compositions is observed, but commonly a symmetrical zoning across carbonate sheets exists (Fig. 3B). The Na–Ca carbonates (mainly shortite) at the rims, near contacts with chlorides forms intergrowths of acicular crystals. The interstitial space between these crystals (at polished surfaces) is either porous or filled with chlorides and aphthitalite $(Na_{0.25}K_{0.75})_2SO_4$. On average the carbonate core is characterised by Na–Ca composition with significant K_2O and SO_3 (Figs. 4, 5; Table 1). Highly variable, but with good correlation, amounts of SO_3 (up to 13 wt.%) and K_2O (up to 14 wt.%) in the individual analyses of core carbonates (Fig. 5) suggest that Na–Ca carbonates are intermixed with tiny aphthitalite crystals, the presence of which can be identified at high magnification (Fig. 3A, area 2), and rare needles of rasvumite (KFe_2S_3). Another Na–Ca carbonate (pirssonite, $Na_2Ca(CO_3)_2{\cdot}2H_2O$) is developed along the cleavage planes in the core and at the contacts with the rims (Fig. 3A-1). In some cases pirssonite replace original Na–Ca carbonate almost completely. It is possible that the original high-temperature alkali carbonate represents a new mineral in the family of Na–Ca carbonates, which includes nyerereite, zemkorite (described in the Udachnaya kimberlites by Egorov et al., 1988) and natro-fairchildite.

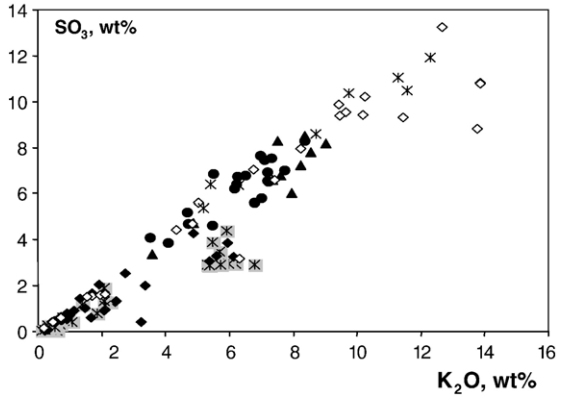

Fig. 5. Covariation of potassium and sulphur abundances in Na–Ca carbonate minerals in sample UV-5a-03. Different symbols represent analytical points in individual sheets.

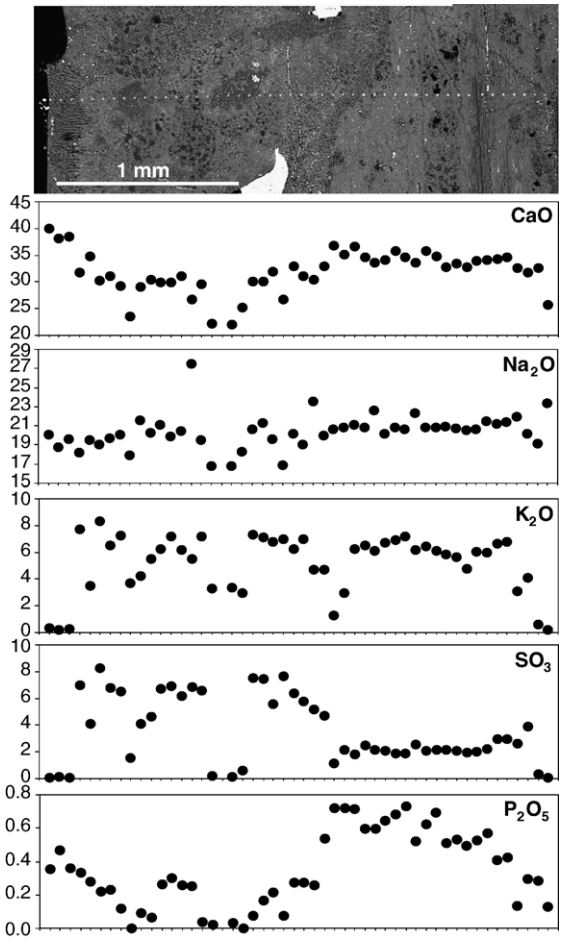

Fig. 4. Compositional variability (in wt.%) across a carbonate sheet in sample UV-5a-03.

An alkali sulphate, aphthitalite $(Na_{0.25}K_{0.75})_2SO_4$, is a minor but widespread component of the carbonate–chloride nodules. It is always associated with halite as irregular blebs, fringing the outmost rims of carbonate sheets (Fig. 3D), and filling fractures and interstitial spaces in carbonates (Fig. 3). As noted before, aphthitalite is also dispersed in the core parts of the carbonate sheets (Fig. 3A, area 2).

Anhydrous and hydrated Na–Ca carbonates with variable Ca/Na ratios are typical in all nodules, but in one sample (UV-2-03) an end-member shortite composition $Na_2Ca_2(CO_3)_3$ was found in close association with Cl-bearing Na–Mg carbonate (northupite $Na_3Mg(CO_3)_2Cl$; Table 1) and calcite. Unlike heterogeneous and thus barely transparent carbonates in other nodules, well-formed crystals of shortite and northupite are clear and can be used for the inclusion studies (see below).

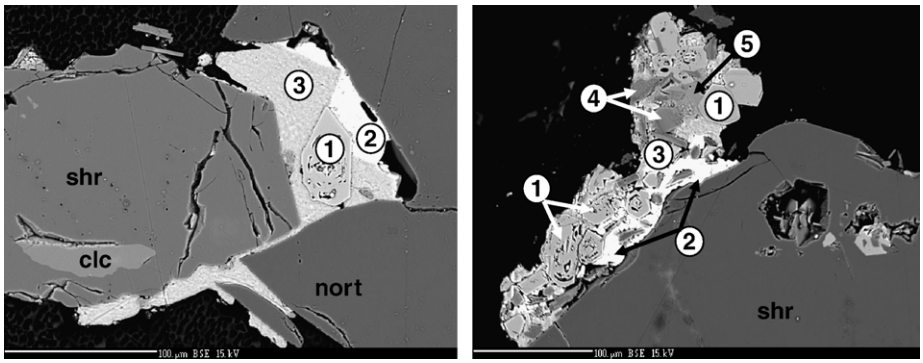

Fig. 6. Euhedral apatite in a chloride–aphthitalite matrix cementing shortite (shr) and nortupite (nort) crystals in sample UV-2-03. 1 — apatite; 2 — sylvite; 3 — halite; 4 — phlogopite; 5 — aphthitalite.

The mineral assemblage in this nodule is very complex (Fig. 6), and includes euhedral crystals of apatite and phlogopite, as well as tetraferriphlogopite, djerfisherite, K–Na and Na–Ca sulphates, Ba-, Ca- and Sr–Ca–Ba-sulphates and carbonates, calcite, perovskite, and bradleyite $Na_3Mg(PO_4)(CO_3)$. The above minerals are present in aggregates within the interstitial chloride cement (Fig. 6) and as inclusions in shortite (Fig. 7).

5. Inclusions in shortite from nodule UV-2-03

Shortite in the nodule UV-2-03 has many inclusions with different sizes, shapes, orientations and compositions (Figs. 7, 8). Most common are mineral inclusions of euhedral apatite, phlogopite–tetraferriphlogopite, northupite and their intergrowths (Fig. 7A–D). These minerals are also present in multiphase inclusions in association with halite, sylvite, K–Na–Ca carbonates and sulphates (Fig. 7C). Zoned apatite contains inclusions of phlogopite, chlorides, alkali–Ca–carbonate and aphthitalite along the growth planes (Fig. 7A, B). Association of euhedral crystal(s) of northupite with halite, sylvite and various sulphates is common within shortite grains (Fig. 7D, F).

Multiphase inclusions of melt (fluid) occur in clusters along healed cracks and growth planes, and are likely to be pseudo-secondary. They have round or cylindric shape, and consist of several (up to eight) translucent crystals, a large vapour bubble and interstitial liquid (Fig. 8A). Daughter crystals show cubic, pseudocubic, hexagonal, pyramidal, and prismatic forms, and some have high relief and birefringence.

Experiments with the multiphase melt (fluid) inclusions in shortite (Fig. 8B) were performed in air using a Linkam TS1500 heating stage. First visible changes to the shape and mutual arrangement of daughter crystals occur at ~170 °C. Heating at >240 °C results in intensive melting and the disappearance of some crystals at 350 °C. At ~390 °C inclusions begin increasing in size, and the remaining daughter minerals melt. At ~400 °C, it appears that at least two liquids are separated from each other by a phase boundary, and the bubble moves back and forth between phases. The inclusions size continues growing. At 415 °C the bubble suddenly disappears, and this coincides with drastic increase in the inclusions size (by the factor of ~4–5 compared to original volume) by melting of the walls. Unfortunately, at this temperature the host shortite lost transparency and started to disintegrate, and heating was stopped. Cooling to room temperature causes inclusions to decrease in size, and inclusion outlines become jagged, possibly because of crystallisation on the walls.

6. Melt inclusions in groundmass olivine

Melt inclusions are trapped either individually within olivine cores and rims, or occur along healed fractures (Golovin et al., 2003; Kamenetsky et al., 2004). Many inclusions are interconnected by thin channels, and thus modifications of original melt compositions by "necking down" cannot be ruled out. Abundant secondary melt inclusions in fractures connected to the groundmass, and decrepitated inclusions, are assumed to have experienced exchange and loss of material, respectively, after entrapment. "Necking down" can explain variable proportions of fluid and mineral phases in the studied melt inclusions. Fluid components are represented by low-density CO_2 bubbles, whereas solid phases are mainly Na–K–Ca carbonates, halite, sylvite, olivine, phlogopite–tetraferriphlopite, calcite, Fe–Ti–Cr oxides, aphthitalite and djerfisherite (Golovin et al., 2003; Sharygin et al., 2003; Kamenetsky et al., 2004). The

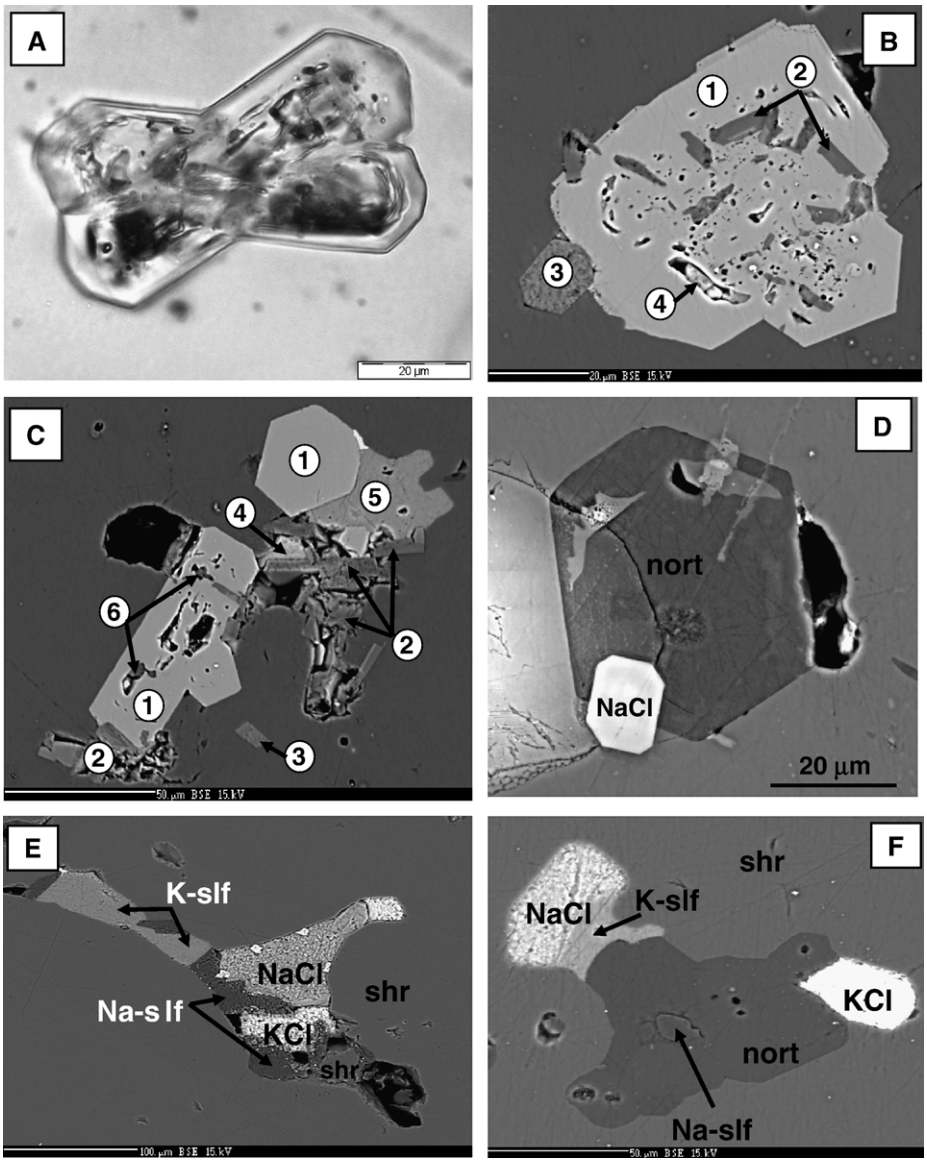

Fig. 7. Mineral and multiphase melt inclusions in shortite (shr) in sample UV-2-03. A — intergrown crystals of zoned apatite; B — zoned apatite (1) with inclusions of phlogopite (2), halite (4) and attached euhedral crystal of tetraferriphlogopite (3); C — euhedral apatite (1) associated with crystallised melt; crystals are represented by phlogopite (2), tetraferriphlogopite (3), halite (4), and aphthitalite (5); note that apatite contains inclusions of phlogopite, chloride minerals and alkali–Ca–carbonate (6); D — inclusion of intergrown euhedral northupite (nort) and halite; E — melt inclusion composed of sulphate (slf) and chloride minerals; F — euhedral northupite inclusion associated with chloride and sulphate minerals.

inclusions occasionally contain monticellite, humite–clinohumite, northupite, clinopyroxene and Ca–Mg–Fe-carbonates.

During heating stage experiments with round, relatively small (40–60 μm) melt inclusions, melting begins at ~160 °C, as indicated by jolting movements of either solid phases or vapour bubbles. The amplitude of bubble movements increases between 420 and 580 °C, indicating the appearance of the liquid phase (melt). Daughter phases experience some changes in their relative position, size and shape at 540–600 °C. At >600 °C we record a number of liquid globules that move freely and change shape continuously. The outline of a single globule is always smoothly curved: it can instantaneously change from spherical to cylindrical, embayed or lopsided, similar to an amoeba. With further heating, the number and size of the globules, as well as the number and size of vapour bubbles, gradually

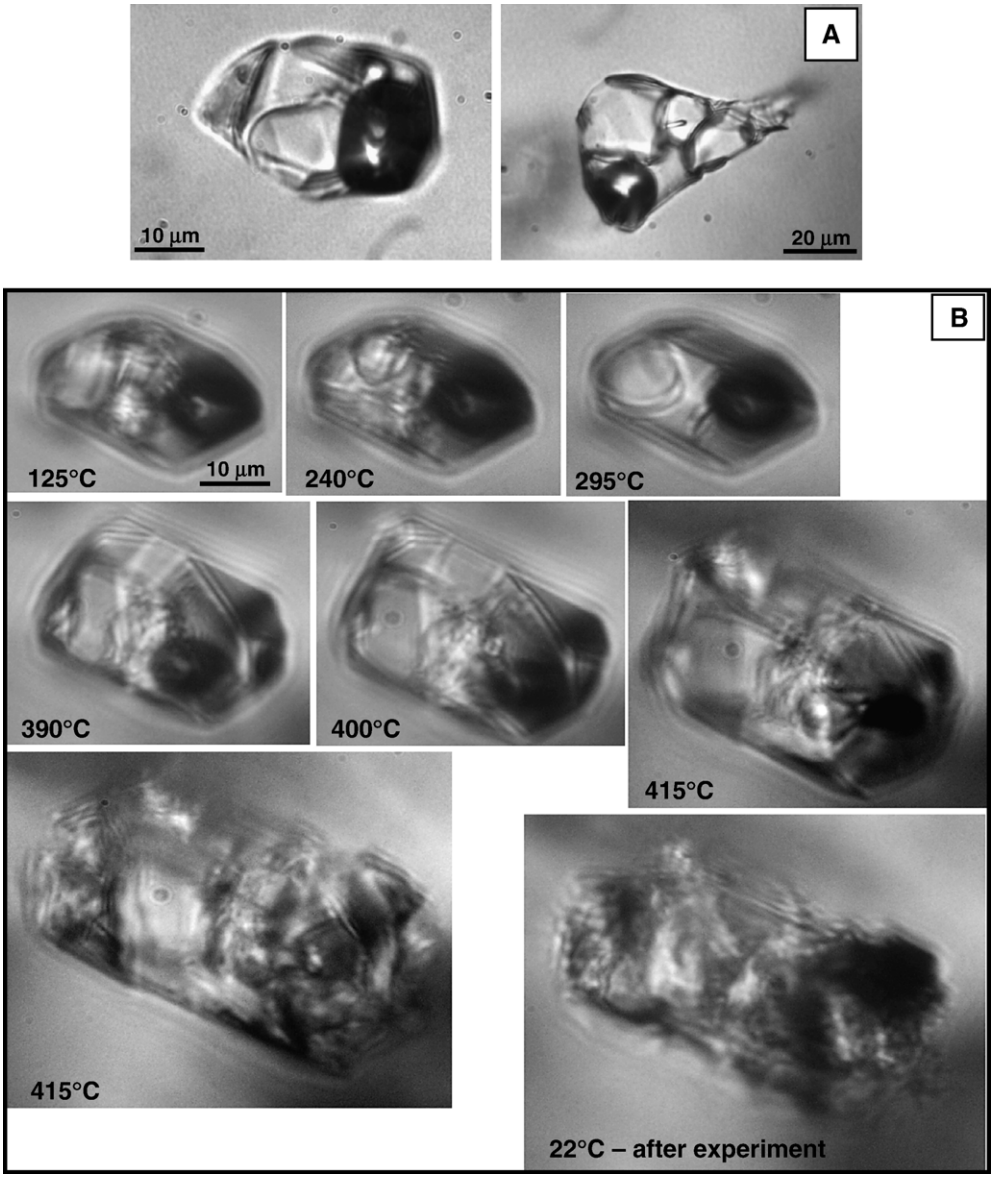

Fig. 8. Multiphase melt inclusions in shortite (sample UV-2-03) at room temperature (A) and during heating experiment (B). Note significant increase of the size of inclusion at $T > 300$ °C (see text for details).

decreases. Homogenisation of the inclusions (except some opaque crystals) occurs when the globules and vapour bubbles disappear almost simultaneously (within 20–30 °C) at 660–760 °C.

During slow cooling (5–20 °C/min), vapour bubbles nucleate at 690–650 °C and then progressively increases in size. Cooling to 610–580 °C, the inclusions acquire a 'foggy" appearance for a split second. We describe this process as the formation of emulsion, i.e, microglobules of liquid in another liquid (carbonate–chloride melt immiscibility). Microglobules coalesce immediately into elongate or sausage-like pinkish globules. The neighbouring globules ("boudins") are subparallel, and are grouped into regularly aligned formations with a common angle of ~75–80° (Fig. 9A). A resemblance to a skeletal or spinifex texture is evident for several seconds, after which the original "pinch-and-swell structure" pulls apart giving rise to individual blebs of melt. The latter coalesce and become spherical with time or further cooling. They continue floating, but slow down with decreasing temperature and further coalescence. The exact moment of crystallisation or complete solidification is not detected.

7. Carbon and oxygen isotope compositions

The carbonate fraction of the Udachnaya-East kimberlite groundmass and carbonates from three chloride–carbonate nodules were analysed for carbon and oxygen isotopes (University of Tasmania, Australia and Institute of Geological and Nuclear Sciences, New Zealand) using a VG Optima Mass Spectrometer equipped with Multiprep system and a Europa GEO 20–20 Mass Spectrometer, equipped with CAPS (automated carbonate machine), respectively. Well-established analytical methods (McCrea, 1950; Sharma and Clayton, 1965) were used for isotope analyses. All measurements (Table 2) are expressed in the familiar delta (δ) notation, in per mil (‰), and normalised to international reference sample (NBS19-Pee Dee Belemnite (VPDB) for carbon and Standard Mean Ocean Water (VSMOW) for oxygen. Precision for carbon isotopes is ±0.05‰ and 0.1‰ for oxygen isotopes.

$\delta^{13}C$ values for the kimberlite carbonate vary insignificantly, from −3.11 to −3.41‰ and are consistent with carbon isotope variations observed in other Udachnaya-East samples (−1.05 to −4.26‰, Galimov and Ukhanov, 1989), kimberlites from the Daldyn–Alakit region (−1.5 to −9.3‰) and Siberian province in general (Galimov and Ukhanov, 1989), magmatic carbonatites ($\delta^{13}C$ values = −2.6 to −7.1‰), diamonds ($\delta^{13}C$ values = −1.9 to −8.8 ‰) and carbonates from other kimberlitic rocks ($\delta^{13}C$ values = −3.3 to −5.7‰, Deines and Gold, 1973; Sheppard and Dawson, 1975; Deines, 1989). $\delta^{18}O$ values of the carbonate fraction of the Udachnaya-East kimberlite range from +12.7 to +14.4‰. These values are systematically lower than those from other Daldyn–Alakit kimberlites (+15.5 to 25.5‰, Galimov and Ukhanov, 1989), but well within the range for carbonates in the group-I kimberlites ($\delta^{18}O$ values = 6.5 to 18.5‰ with a strong maximum at about 12‰; Deines and Gold, 1973; Kobelski et al., 1979; Deines, 1989; Price et al., 2000; Fedortchouk and Canil, 2004) and carbonates from magmatic carbonatites ($\delta^{18}O$ = 4.5 to 28‰; Deines and Gold, 1973).

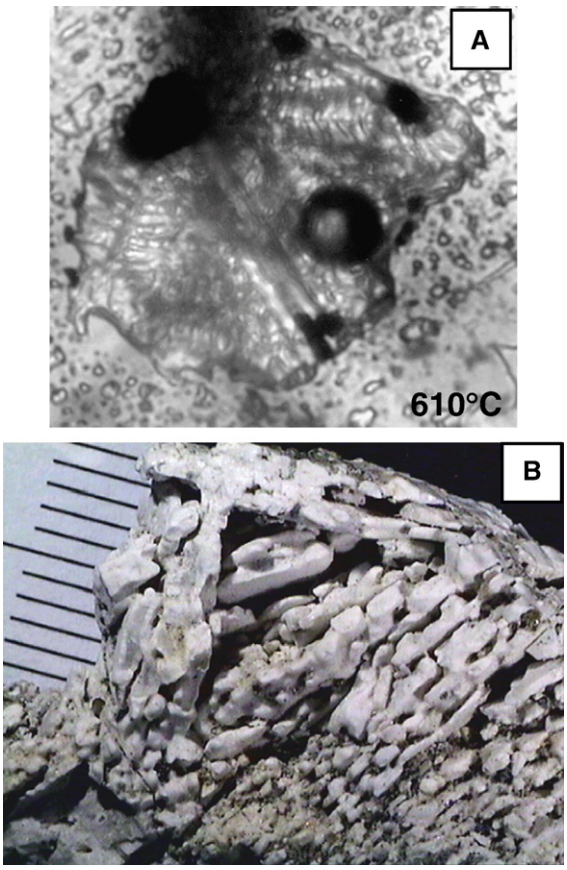

Fig. 9. Textural similarity between olivine-hosted melt inclusion at the moment of immiscibility (A) and chloride–carbonate nodule, sample UV-5a-03 (B).

Table 2
Stable isotope composition of host kimberlite and chloride–carbonate nodules

	$\delta^{18}O$ ‰ SMOW	$\delta^{13}C$ ‰ PDB
Chloride–carbonate nodules		
UV-1-03	12.47	−3.73
UV-2-03	13.90	−2.68
UV-5a-03	12.27	−3.72
Kimberlite groundmass carbonates[a]		
YBK-0	12.87	−3.35
YBK-1	13.78	−3.28
YBK-3	13.68	−3.22

[a] Average of two determinations.

$\delta^{13}C$ (−2.67 to −3.73 ‰) and $\delta^{18}O$ (12.3 to 13.9 ‰) values for carbonates in the chloride–carbonate nodules have a small variability and are consistent with those of the carbonate component of the host kimberlite groundmass and kimberlites worldwide (Deines and Gold, 1973; Kobelski et al., 1979; Mitchell, 1986; Deines, 1989; Kirkley et al., 1989; Price et al., 2000; Fedortchouk and Canil, 2004).

8. Discussion and conclusions

8.1. Chloride–carbonate nodules are samples of residual kimberlite magma

The presence of the chloride–carbonate nodules in the Udachnaya-East kimberlite is significant in several aspects. Firstly, such nodules have not been reported to

date in any other known kimberlite rock. Secondly, their host kimberlite shows unprecedented enrichment in alkali chloride and alkali carbonate components (Kamenetsky et al., 2004; Maas et al., 2005). Thirdly, their host kimberlite is completely unaltered (Marshintsev et al., 1976; Marshintsev, 1986; Kamenetsky et al., 2004), and this feature taken together with very low measured H_2O content (<0.5 wt.%) is unique for kimberlites worldwide. The degree of serpentinisation within the Udachnaya-East body gradually decreases with depth, and finally serpentine disappears (Zinchuk et al., 1993). This is concomitant with an increase in unaltered olivine, carbonate in the groundmass, and concentrations of K_2O and Cl, and generally unaltered nature of xenoliths (Pavlov and Ilupin, 1973; Zinchuk et al., 1993). All these facts are consistent with a flushing of either magmatic or meteoric aqueous fluids through kimberlites (Drozdov et al., 1989) which would cause dissolution of chloride minerals and serpentinisation.

Magmatic shortite was first discovered in the kimberlite of Ontario, which was characterised by "*the extensive preservation of fresh olivine…and general absence of hydrothermal effects on the megacrysts, groundmass, or host rocks*" (Watkinson and Chao, 1973). Similar unaltered samples from Udachnaya-East indicate that the absence of "ephemeral" minerals, like shortite and chlorides, in common kimberlites can be related to their pervasive alteration. It is also possible that these minerals still remain in smaller than original quantities in altered kimberlites, but require special effort and sample preparation for recognition.

The textural relationships between chloride–carbonate nodules and kimberlite groundmass do not indicate a chemical and/or thermometamorphic reaction at the contacts. Importantly, alkali carbonate and chloride minerals, comprising the kimberlite groundmass and melt inclusions in olivine (Golovin et al., 2003; Kamenetsky et al., 2004), are compositionally similar to these minerals in the nodules. Moreover, the C and O isotope values of carbonates from the chloride–carbonate nodules and carbonate fraction of three fresh studied samples of the Udachnaya-East kimberlite are also comparable to each other (Table 2). Thus, a xenogenic origin for the nodules (e.g., from country sedimentary rocks) is highly unlikely. We consider that a prolonged evolution of the kimberlite magma by olivine crystallisation was responsible for a build-up of abundances of alkalies, chloride, carbonate, and sulphate components. As a result, the residual kimberlite magma acquires essentially a non-silicate composition that is represented by abundant chloride, carbonate and other Cl- and S-bearing minerals in the groundmass. The non-silicate residual kimberlite magma has low temperatures (<650–750 °C), as shown by the study of the Udachnaya-East melt inclusions (Kamenetsky et al., 2004), experimental data on the fluorine-bearing Na_2CO_3–$CaCO_3$ system (Jago and Gittins, 1991) and direct temperature measurements in the halogen-rich (up to 15 wt.% F+Cl, Jago and Gittins, 1991) natrocarbonatite lava lakes and flows of the Oldoinyo Lengai volcano (Krafft and Keller, 1989; Dawson et al., 1990; Keller and Krafft, 1990). However, even at these temperatures it is highly fluid. Thus, we envisage that droplets of residual melt separate from a solid aluminosilicate framework of the magma, percolate into weaker, less solidified zones, and finally coalesce, forming melt pockets. The latter are now seen in the kimberlite as chloride–carbonate nodules.

8.2. Liquid immiscibility and crystallisation of residual kimberlite magma

Liquid immiscibility is observed in the olivine-hosted melt inclusions at ~600 °C on cooling (Fig. 9A; see also Kamenetsky et al., 2004). The immiscible liquids are recognized as the carbonate and chloride on the basis that these minerals are dominantly present in the unheated melt inclusions (Golovin et al., 2003; Kamenetsky et al., 2004). Remarkable textures, observed in melt inclusions at the exact moment of melt unmixing (Fig. 9A), is governed by the carbonate crystallographic properties. The presence of similar textures in the chloride–carbonate nodules (Figs. 2A, 9B) is unambiguous "snapshot" record of the chloride–carbonate melt immiscibility in rocks. Chloride–sulphate microveinlets in carbonates (Fig. 3) suggest intruding of already rigid carbonate by still liquid or plastic material, and this additionally supports earlier event of carbonate–chloride–sulphate immiscibility. The previous natural evidence was based on melt and fluid inclusions in the skarn minerals of Mt Vesuvius (Fulignati et al., 2001), minerals composing olivine–melilite–monticellite rocks from the Krestovskiy massif, Siberia (Panina, 2005) and kimberlitic diamonds (Bulanova et al., 1998; Izraeli et al., 2001; Izraeli et al., 2004; Klein-BenDavid et al., 2004). However, the extensive review of experimental studies (Veksler, 2004) points to the lack of data for chloride–carbonate systems.

Given the analogy with the texture of melt inclusions at the onset of immiscibility, the boudin-like shape of the carbonate sheets and their subparallel alignment, argues for preservation of primary (instantaneous) immiscibility texture. This means that post-immiscibility (<600 °C) cooling and crystallisation were fast enough to prevent aggregation of one of the immiscible liquids into ovoid or spherical globules that are more typical of steady-state

immiscibility. Occurrence of the chloride-rich veinlets in the carbonate sheets (Fig. 3) testifies to later solidification of the chloride liquid relative to carbonate crystallisation. The round and ameboid-like bleb textures of sylvite in halite (Fig. 3) are also reminiscent of liquid immiscibility. In theory this contradicts the fact of complete miscibility in the system NaCl–KCl above the eutectic point of ~660 °C. However, the separation of the Na–K chloride melt from the carbonatitic melt, in the case of Udachnaya-East residual melt pockets, occurred at temperatures below the eutectic, and thus the chloride liquid was supercooled. On the other hand, it was close to the point of solid solution unmixing in the system 75% NaCl–25% KCl (543 °C at 1 atm), and in this case unmixing of liquids rather than solids is more likely.

Crystallisation from a homogeneous chloride–carbonate liquid (i.e., prior to immiscibility) is possible, and very unusual Na–Mg carbonates containing an NaCl molecule (northupite $NaCl*Na_2Mg(CO_3)_2$) is an example (Table 1). Disruption of the melt structure caused by chloride–carbonate immiscibility and followed by reduction in solubility of the phosphate and Fe–Mg aluminosilicate components, prompted rapid crystallisation of zoned and often skeletal micro-crystals of apatite and phlogopite–tetraferriphlogopite (Fig. 6). Fibrous aggregates of phlogopite in carbonates (Fig. 10A) and sylvite (Fig. 10B) are common and suggestive of incomplete extraction of the aluminosilicate component from carbonate and chloride melts by post-immiscibility crystallisation. After chloride–carbonate liquid unmixing the sulphate component of the original melt was largely accommodated within the carbonate melt. It was partially released as an aphthitalite melt at the chloride–carbonate interfaces, leaving porous K- and S-free carbonate behind (Fig. 3B), and it was also partially exsolved and re-distributed within the carbonate (Fig. 3A) at subsolidus temperatures.

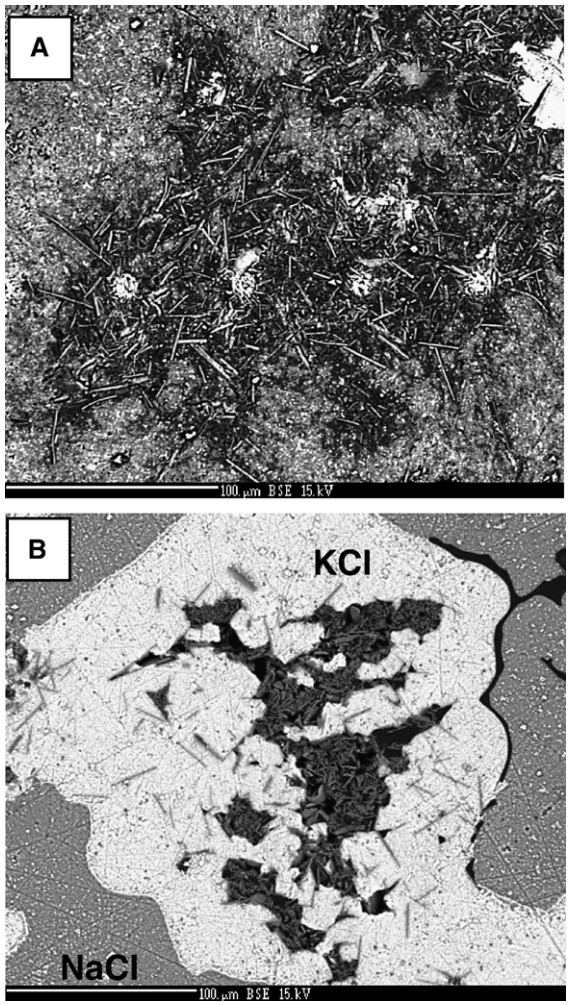

Fig. 10. Fibrous phlogopite crystal aggregates in alkali carbonate (A) and sylvite (B); sample UV-5a-03.

8.3. Possible origins of chlorine enrichment

The studied Udachnaya-East kimberlite is unusually enriched in chlorine and alkalies, yet it is essentially anhydrous (Table 1). Its groundmass and residual melt pockets are dominated by minerals (Table 1) unknown elsewhere, or found rarely as magmatic minerals, but in paragenetic association with common silicates and oxides. The alkali chloride–carbonate liquid results from exhaustion of silicate components in the kimberlite magma. It pools at <700 °C, undergoes immiscibility at ~600 °C (Fig. 9) and solidifies at even lower temperatures, possibly 300–400 °C. The unusual mineralogy and compositions together with the lowest temperatures and viscosities, yet found for terrestrial melts, make a perfect analogy with the Oldoinyo Lengai carbonatites, and with melt inclusions in minerals from ultramafic alkaline and carbonatitic complexes (Veksler et al., 1998; Zaitsev and Chakhmouradian, 2002; Panina, 2005).

Although the Oldoinyo Lengai carbonatite lavas are indisputable magmatic, the ultimate source of the natrocarbonate and halogen components is still a matter of significant controversy (see review in Nielsen and Veksler, 2002). One of the possible origins through melting of regional troniferous sediments has been advocated (Milton, 1968), but later rejected on the basis of petrological and geochemical data (Bell and Dawson, 1995). The presence of extensive carbonate–evaporite basin in the south and southwest of the Siberian craton also pose a possibility of contamination of the

Udachnaya kimberlite magma en route to the surface. Obviously, the difficulty in resolving this question using stable and radiogenic isotopes is in that very small amount of evaporitic chloride (~5 wt.%) can account for the Cl enrichment in the Udachnaya-East kimberlite and effects of isotope fractionation between magmatic minerals at low temperatures remain unknown.

A number of considerations, although speculative to some extent, allow us to argue against contamination in this case:

- The Udachanya pipes were emplaced through the Lower to Middle Cambrian sediments of the Anabar–Sinyaya transitional belt, separating the north-eastern Yudoma–Olenek belt of normal marine carbonate facies and the south-western Turukhansk–Irkutsk–Olekma belt of carbonate–evaporite facies (Brasier and Sukhov, 1998). The Anabar–Sinyaya transitional belt of archaeocyathan–microbial facies comprises shallow marine shoals with calcimicrobe bioherms, but no evaporates have been found in numerous boreholes (from 700 to 1700 m deep) around the Udachnaya pipes.
- Extensive mining and drilling (~1000 m) of the Udachnaya pipe have not, to date, encountered evaporites within the country rocks, evaporite-related fragments or xenoliths in the kimberlite (Zinchuk et al., 1993).
- The fresh kimberlites of the Udachnaya-East pipe belong to the latest stages of emplacement (Zinchuk et al., 1993), and thus because of established magmatic conduits the interaction of magmas en route to the surface with crustal sediments seems unlikely.
- According to radiogenic isotopes (Maas et al., 2005) the studied kimberlite remained a closed system since emplacement. This is independently supported by the fact of spontaneous outgassing (~10^5 m^3/day; 50–70 atm; Drozdov et al., 1989) of pristine magmatic H_2, N_2 and CH_4 (Marshintsev, 1986) from boreholes drilled through this unaltered block of the Udachnaya-East kimberlite.
- The minerals that are present in the Udachnaya-East kimberlite and that signify high concentrations of alkalies and chlorine in kimberlite magmas have been reported from other kimberlites; for example, halite (Mir pipe, Yakutia, Pavlov and Ilupin, 1973), shortite (the Upper Canada Gold Mine, Ontario, Watkinson and Chao, 1973), zemkorite ($Na_{1.77}K_{0.29}$)$Ca_{1.08}(CO_3)_{1.95}$ (Venkatampalle, southern India, Parthasarathy et al., 2002), and Cl-bearing K–Fe sulphide, djerfisherite (Yakutian kimberlites (Dobrovol'skaya et al., 1975); Frank Smith mine, South Africa (Clarke et al., 1977); Elwin Bay, Somerset Island, Canada (Clarke et al., 1994)).
- Occurrence of alkali- and Cl-rich phases in melt inclusions in the deep formed olivine cores and Cr-diopside and among alteration products of mantle xenocrysts (garnet, pyroxenes and ilmenite), and presence of similar minerals in the kimberlites worldwide. Similar alteration assemblage of eclogite xenoliths in the Udachnaya kimberlites was ascribed to a metasomatic event that occurred in the upper mantle, after the xenoliths were incorporated in the kimberlite (Misra et al., 2004).
- Discoveries of halite and sylvite (Zolensky et al., 1999) and djerfisherite (Fuchs, 1966) in chondrites reinforce origin of these minerals in Udachnaya and other kimberlites from mantle-derived components.

We emphasise that in the Udachnaya-East kimberlite the combination of extraordinary freshness, high abundances of Na, K and Cl, depletion in H_2O, and preservation of water-soluble minerals and chloride–carbonate melt pockets cannot be coincidental. We believe that these features are inherently related. This is independently confirmed by the study of the Oldoinyo Lengai magmas: "*…the presence of so much Cl is further evidence that the magma was dry, because an aqueous fluid would have removed it. …Because the magma is dry, no aqueous fluid develops; alkalis, therefore, are not removed but are progressively concentrated in the magma by continued fractionation of essentially alkali-free minerals*" (Gittins, 1989).

From the analogy with dry carbonatite magmas of Oldoinyo Lengai (Keller and Krafft, 1990; Keller and Spettel, 1995) and experimental evidence that alkali carbonatite magmas "*will persist only if the magma is dry*" (Cooper et al., 1975) we conclude that the parental magma of the studied kimberlite was essentially anhydrous and carbonate-rich. This is indirectly supported by the spectroscopic study of micro-inclusions in Udachnaya cubic diamonds that showed that their parental media was an H_2O-poor carbonatitic melt (Zedgenizov et al., 2004).

Chlorine and H_2O show opposing solubilities in fluid-saturated silicate melts, as they apparently compete for similar structural positions in the melt (Webster et al., 1999; Chevychelov et al., 2003). Although Cl does not form complexes with Si in a melt, it may complex with network modifier cations, especially the alkalies, Ca and Mg (Carroll and Webster, 1994; Sandland et al., 2004). General "dryness" of carbonatites and enrichment of natrocarbonatites in halogens (Gittins, 1989; Keller and Krafft, 1990; Jago and Gittins,

1991; Dawson et al., 1995) suggest that Cl and H_2O decouple which can be an intrinsic feature of carbonate-rich kimberlite magmas. If this is the case, the conventional role of H_2O in governing low temperatures and low viscosities of kimberlite magmas can be readdressed to Cl. Furthermore, the data on carbonate–chloride compositions of melt inclusions in diamonds (Bulanova et al., 1998; Izraeli et al., 2001; Izraeli et al., 2004; Klein-BenDavid et al., 2004), nucleation and growth of diamonds in alkaline carbonate melts (Pal'yanov et al., 2002) and catalytic effect of Cl on the growth of diamonds in the system C–K_2CO_3–KCl (Tomlinson et al., 2004) concur with the proposed mantle origin of chloride and alkali carbonate components in the Udachnaya-East kimberlite. Chlorides, discovered in the Monahans (1998) chondrite immediately after its fall (Zolensky et al., 1999), suggest that the Cl content in the Earth's undepleted mantle can be largely underestimated.

Acknowledgements

We thank Phil Robinson, Sarah Gilbert, Katie McGoldrick, and Graham Rowbottom for their assistance with analytical work. We are grateful to Alex Sobolev, Roland Maas, David Green, Barry Dawson, Oded Navon, Lia Panina and Wally Herrmann for discussions and corrections. The manuscript was improved based on comments and suggestions from Ilya Veksler and an anonymous reviewer. We are grateful to Maria Luce Frezzotti for organising E.C.R.O.F.I. XVIII conference in Siena, inviting this presentation and editorial handling of the manuscript. V.S.K. is supported by an Australian Research Council Professorial Fellowship and Discovery Grant, and M.B.K. acknowledges receipt of an Australian Postgraduate Scholarship.

References

Becker, M., le Roex, A.P., 2006. Geochemistry of South African on- and off-craton, Group I and Group II kimberlites: petrogenesis and source region evolution. J. Petrol. 47, 673–703.

Bell, K., Dawson, J.B., 1995. An assessment of the alleged role of evaporites and saline brines in the origin of natrocarbonatites. In: Bell, K., Keller, J. (Eds.), Carbonatite Volcanism: Oldoinyo Lengai and Petrogenesis of Natrocarbonatites. Springer-Verlag, pp. 137–147.

Bogatikov, O.A., Kononova, V.A., Golubeva, Y.Y., Zinchuk, N.N., Ilupin, I.P., Rotman, A.Y., Levsky, L.K., Ovchinnikova, G.V., Kondrashov, I.A., 2004. Variations in chemical and isotopic compositions of the Yakutian kimberlites and their causes. Geochem. Int. 42, 799–821.

Brasier, M.D., Sukhov, S.S., 1998. The falling amplitude of carbon isotopic oscillations through the lower to middle Cambrian: northern Siberia data. Can. J. Earth Sci. 35, 353–373.

Bulanova, G.P., Griffin, W.J., Ryan, C.G., 1998. Nucleation environment of diamonds from Yakutian kimberlites. Mineral. Mag. 62, 409–419.

Burgess, R., Turner, G., Harris, J.W., 1992. ^{40}Ar–^{39}Ar laser probe studies of clinopyroxene inclusions in eclogitic diamonds. Geochim. Cosmochim. Acta 56, 389–402.

Carroll, M.R., Webster, J.D., 1994. Solubilities of sulfur, noble gases, nitrogen, chlorine, and fluorine in magmas. In: Carroll, M.R., Holloway, J.R. (Eds.), Volatiles in Magmas. Reviews in Mineralogy. Mineralogical Society of America, Washington, pp. 231–279.

Chevychelov, V.Y., Simakin, A.G., Bondarenko, G.V., 2003. Mechanism of chlorine dissolution in water-saturated model granodiorite melt: applications of IR spectroscopic methods. Geochem. Int. 41, 395–409.

Clarke, M.G.C., Roberts, B., 1986. Carbonated melilitites and calcitized alkalicarbonatites from Homa Mountain, western Kenya: a reinterpretation. Geol. Mag. 123, 683–692.

Clarke, D.B., Pe, G.G., Mackay, R.M., Gill, K.R., O'Hara, M.J., Gard, J.A., 1977. A new potassium–iron–nickel sulphide from a nodule in kimberlite. Earth Planet. Sci. Lett. 35, 421–428.

Clarke, D.B., Mitchell, R.H., Chapman, C.A.T., MacKay, R.M., 1994. Occurrence and origin of djerfisherite from the Elwin Bay kimberlite. Somerset Island, Northwest Territories. Can. Mineral. 32, 815–823.

Clement, C.R., Skinner, E.M.W., Scott Smith, B.H., 1984. Kimberlite re-defined. J. Geol. 32, 223–228.

Cooper, A.F., Gittins, J., Tuttle, O.F., 1975. The system Na_2CO_3–K_2CO_3–$CaCO_3$ at 1 kilobar and its significance in carbonatite petrogenesis. Am. J. Sci. 275, 534–560.

Dawson, J.B., 1962. The geology of Oldoinyo Lengai. Bull. Volcanol. 24, 349–387.

Dawson, J.B., 1989. Sodium carbonatite extrusions from Oldoinyo Lengai, Tanzania: implications for carbonatite complex genesis. In: Bell, K. (Ed.), Carbonatites. Genesis and Evolution. Unwin Hyman, London, pp. 255–277.

Dawson, J.B., Garson, M.S., Roberts, B., 1987. Altered former alkalic carbonatite lava from Oldoinyo Lengai, Tanzania: inferences for calcite carbonatite lavas. Geology 15, 765–768.

Dawson, J.B., Pinkerton, H., Norton, G.E., Pyle, D.M., 1990. Physicochemical properties of alkali carbonatite lavas: data from the 1988 Eruption of Oldoinyo Lengai, Tanzania. Geology 18, 260–263.

Dawson, J.B., Pinkerton, H., Norton, G.E., Pyle, D.M., Browning, P., Jackson, D., Fallick, A.E., 1995. Petrology and geochemistry of Oldoinyo Lengai lavas extruded in November 1988: magma source, ascent and crystallization. In: Bell, K., Keller, J. (Eds.), Carbonatite Volcanism: Oldoinyo Lengai and Petrogenesis of Natrocarbonatites. Springer-Verlag, pp. 47–69.

Deans, T., Roberts, B., 1984. Carbonatite tuffs and lava clasts of the Tinderet foothills, western Kenya: a study of calcified natrocarbonatites. J. Geol. Soc. (Lond.) 141, 563–580.

Deines, P., 1989. Stable isotope variations in carbonatites. In: Bell, K. (Ed.), Carbonatites. Genesis and Evolution. Unwin Hyman, London, pp. 301–359.

Deines, P., Gold, D.P., 1973. The isotopic composition of carbonatite and kimberlite carbonates and their bearing on the isotopic composition of deep-seated carbon. Geochim. Cosmochim. Acta 37, 1709–1733.

Dobrovol'skaya, M.G., Tsepin, A.I., Ilupin, I.P., Ponomarenko, A.I., 1975. Djerfisherite from the kimberlites of Yakutia. In: Tatarinov, P.M. (Ed.), Paragenesis of Minerals in Magmatic Deposits. Nauka, Leningrad, Russia, pp. 3–11.

Drozdov, A.V., Egorov, K.N., Gotovtsev, S.P., Klimovsky, I.V., 1989. Hydrogeological structure and hydrochemical zonation of the Udachnaya kimberlite pipe. In: Anisimova, N.P. (Ed.), Combined Permafrost and Hydrogeological Studies. Institute of Permafrost, Siberian Branch of Academy of Sciences, Yakutsk, pp. 146–155.

Egorov, K.N., Ushchapovskaia, Z.F., Kashaev, A.A., Bogdanov, G.V., Sizykh, I.I., 1988. Zemkorite — a new carbonate from Yakutian kimberlites. Dokl. Akad. Nauk SSSR 301, 188–192.

Fedortchouk, Y., Canil, D., 2004. Intensive variables in kimberlite magmas, Lac de Gras, Canada and implications for diamond survival. J. Petrol. 45, 1725–1745.

Fraser, K.J., Hawkesworth, C.J., Erlank, A.J., Mitchel, R.H., Scott-Smith, B.H., 1985. Sr, Nd, and Pb isotope and minor element geochemistry of lamproites and kimberlites. Earth Planet. Sci. Lett. 76, 57–70.

Fuchs, L.H., 1966. Djersherite, alkali copper–iron sulfide: a new mineral from enstatite chondrites. Science 153, 166–167.

Fulignati, P., Kamenetsky, V.S., Marianelli, P., Sbrana, A., Mernagh, T.P., 2001. Melt inclusion record of immiscibility between silicate, hydrosaline and carbonate melts: applications to skarn genesis at Mount Vesuvius. Geology 29, 1043–1046.

Galimov, E.M., Ukhanov, A.V., 1989. Nature of carbonate component of kimberlites. Geokhimiya 3, 337–348.

Gittins, J., 1989. The origin and evolution of carbonatite magmas. In: Bell, K. (Ed.), Carbonatites. Genesis and Evolution. Unwin Hyman, London, pp. 580–599.

Gittins, J., McKie, D., 1980. Alkalic carbonatite magmas: Oldoinyo Lengai and its wider applicability. Lithos 13, 213–215.

Golovin, A.V., Sharygin, V.V., Pokhilenko, L.N., Mal'kovets, V.G., Kolesov, B.A., Sobolev, N.V., 2003. Secondary melt inclusions in olivine from unaltered kimberlites of the Udachnaya-East pipe, Yakutia. Trans. (Doklady) Russ. Acad. Sci. 388, 93–96.

Harris, M., le Roex, A., Class, C., 2004. Geochemistry of the Uintjiesberg kimberlite, South Africa: petrogenesis of an off-craton, group I, kimberlite. Lithos 74, 149–165.

Hay, R.L., 1983. Natrocarbonatite tephra of Kerimasi volcano, Tanzania. Geology 11, 599–602.

Izraeli, E.S., Harris, J.W., Navon, O., 2001. Brine inclusions in diamonds: a new upper mantle fluid. Earth Planet. Sci. Lett. 187, 323–332.

Izraeli, E.S., Harris, J.W., Navon, O., 2004. Fluid and mineral inclusions in cloudy diamonds from Koffiefontein, South Africa. Geochim. Cosmochim. Acta 68, 2561–2575.

Jago, B.C., Gittins, J., 1991. The role of fluorine in carbonatite magma evolution. Nature 349, 56–58.

Kamenetsky, M.B., Sobolev, A.V., Kamenetsky, V.S., Maas, R., Danyushevsky, L.V., Thomas, R., Sobolev, N.V., Pokhilenko, N.P., 2004. Kimberlite melts rich in alkali chlorides and carbonates: a potent metasomatic agent in the mantle. Geology 32, 845–848.

Keller, J., Krafft, M., 1990. Effusive natrocarbonatite activity of Oldoinyo Lengai, June 1988. Bull. Volcanol. 52, 629–645.

Keller, J., Spettel, B., 1995. The trace element compositions and petrogenesis of natrocarbonatites. In: Bell, K., Keller, J. (Eds.), Carbonatite Volcanism: Oldoinyo Lengai and Petrogenesis of Natrocarbonatites. Springer-Verlag, pp. 70–86.

Kinny, P.D., Griffin, W.L., Heaman, L.M., Brakhfogel, F.F., Spetsius, Z.V., 1997. SHRIMP U–Pb ages of perovskite from Yakutian kimberlites. Russ. Geol. Geophys. 38, 91–99.

Kirkley, M.B., Smith, H.S., Gurney, J.J., 1989. Kimberlite carbonates — a carbon and oxygen stable isotope study. In: Ross, J., et al. (Ed.), Kimberlites and Related Rocks: Their Composition, Occurrence, Origin and Emplacement, vol. 1. Blackwell Scientific Publications, Sydney, pp. 264–281.

Klein-BenDavid, O., Izraeli, E.S., Hauri, E.H., Navon, O., 2004. Mantle fluid evolution — a tale of one diamond. Lithos 77, 243–253.

Kobelski, B.J., Gold, D.P., Deines, P., 1979. Variations in stable isotope compositions for carbon and oxygen in some South African and Lesothan kimberlites. In: Boyd, F.R., Meyer, H.O.A. (Eds.), Kimberlites, Diatremes and Diamonds: Their Geology, Petrology, and Geochemistry. American Geophysical Union, Washington, DC, pp. 252–271.

Krafft, M., Keller, J., 1989. Temperature measurements in carbonatite lava lakes and flows from Oldoinyo Lengai, Tanzania. Science 245, 168–170.

le Roex, A.P., Bell, D.R., Davis, P., 2003. Petrogenesis of group I kimberlites from Kimberley, South Africa: evidence from bulk-rock geochemistry. J. Petrol. 44, 2261–2286.

Maas, R., Kamenetsky, M.B., Sobolev, A.V., Kamenetsky, V.S., Sobolev, N.V., 2005. Sr, Nd, and Pb isotope evidence for a mantle origin of alkali chlorides and carbonates in the Udachnaya kimberlite, Siberia. Geology 33, 549–552.

Mal'kov, B.A., Bobolovich, G.N., 1977. Genesis of kimberlite as shown by study of inclusions in calcite and apatite. Trans. (Dokl.) USSR Acad. Sci., Earth Sci. Sect. 234, 181–183.

Marshintsev, V.K., 1986. Vertical Heterogeneity of Kimberlite Bodies in Yakutiya. Nauka, Novosibirsk. 239 pp.

Marshintsev, V.K., Migalkin, K.N., Nikolaev, N.C., Barashkov, Y.P., 1976. Unaltered kimberlite of the Udachnaya East pipe. Trans. (Dokl.) USSR Acad. Sci., Earth Sci. Sect. 231, 961–964.

Maslovskaja, M.N., Yegorov, K.N., Kolosnitsyna, T.I., Brandt, S.B., 1983. Strontium isotope composition, Rb–Sr absolute age, and rare alkalies in micas from Yakutian kimberlites. Trans. (Dokl.) USSR Acad. Sci., Earth Sci. Sect. 266, 451–455.

McCrea, J.M., 1950. On the isotopic chemistry of carbonates and a paleotemperature scale. J. Chem. Phys. 18, 849–857.

Milton, C., 1968. The "Natro-Carbonatite Lava" of Oldoinyo Lengai, Tanzania. Geol. Soc. Am., Spec. Pap. 121, 202.

Misra, K.C., Anand, M., Taylor, L.A., Sobolev, N.V., 2004. Multi-stage metasomatism of diamondiferous eclogite xenoliths from the Udachnaya kimberlite pipe, Yakutia, Siberia. Contrib. Mineral. Petrol. 146, 696–714.

Mitchell, R.H., 1986. Kimberlites: Mineralogy, Geochemistry and Petrology. Plenum Press, New York. 442 pp.

Mitchell, R.H., 1989. Aspects of the petrology of kimberlites and lamproites: some definitions and distinctions. In: Ross, J., et al. (Eds.), Kimberlites and Related Rocks: Their Composition, Occurrence, Origin and Emplacement. Blackwell Scientific Publications, Sydney, pp. 7–45.

Nielsen, T.F.D., Veksler, I.V., 2002. Is natrocarbonatite a cognate fluid condensate? Contrib. Mineral. Petrol. 142, 425–435.

Pal'yanov, Y.N., Sokol, A.G., Borzdov, Y.M., Khokhryakov, A.F., 2002. Fluid-bearing alkaline carbonate melts as the medium for the formation of diamonds in the Earth's mantle: an experimental study. Lithos 60, 145–159.

Panina, L.I., 2005. Multiphase carbonate–salt immiscibility in carbonatite melts: data on melt inclusions from the Krestovskiy massif minerals (Polar Siberia). Contrib. Mineral. Petrol. 150, 19–36.

Parthasarathy, G., Chetty, T.R.K., Haggerty, S.E., 2002. Thermal stability and spectroscopic studies of zemkorite: a carbonate from the Venkatampalle kimberlite of southern India. Am. Mineral. 87, 1384–1389.

Pasteris, J.D., 1984. Kimberlites: complex mantle melts. Annu. Rev. Earth Planet. Sci. 12, 133–153.

Pavlov, D.I., Ilupin, I.P., 1973. Halite in Yakutian kimberlite, its relations to serpentine and the source of its parent solutions. Trans. (Dokl.) USSR Acad. Sci., Earth Sci. Sect. 213, 178–180.

Price, S.E., Russell, J.K., Kopylova, M.G., 2000. Primitive magma from the Jericho Pipe, NWT, Canada: constraints on primary kimberlite melt chemistry. J. Petrol. 41, 789–808.

Sandland, T.O., Du, L.-S., Stebbins, J.F., Webster, J.D., 2004. Structure of Cl-containing silicate and aluminosilicate glasses: a ^{35}Cl MAS-NMR study. Geochim. Cosmochim. Acta 68, 5059–5069.

Sharma, T., Clayton, R.N., 1965. Measurement of $^{18}O/^{16}O$ ratios of total oxygen in carbonates. Geochim. Cosmochim. Acta 29, 1347–1353.

Sharygin, V.V., Golovin, A.V., Pokhilenko, N.P., Sobolev, N.V., 2003. Djerfisherite in unaltered kimberlites of the Udachnaya-East pipe, Yakutia. Trans. (Dokl.) Russian Acad. Sci., Earth Sci. Sect. 390, 554–557.

Sheppard, S.M.F., Dawson, J.B., 1975. Hydrogen, carbon and oxygen isotope studies of megacryst and matrix minerals from Lesothan and South African kimberlites. Phys. Chem. Earth 9, 747–763.

Skinner, E.M.W., Clement, C.R., 1979. Mineralogical classification of Southern African kimberlites. In: Boyd, F.R., Meyer, H.O.A. (Eds.), Kimberlites, Diatremes and Diamonds: Their Geology, Petrology and Geochemistry. American Geophysical Union, Washington, D.C., pp. 129–139.

Smith, C.B., 1983. Pb, Sr and Nd isotopic evidence for sources of southern African Cretaceous kimberlites. Nature 304, 51–54.

Smith, C.B., Gurney, J.J., Skinner, E.M.W., Clement, C.R., Ebrahim, N., 1985. Geochemical character of the southern African kimberlites: a new approach based on isotopic constraints. Trans. Geol. Soc. S. Afr. 88, 267–280.

Sobolev, A.V., Sobolev, N.V., Smith, C.B., Dubessy, J., 1989. Fluid and melt compositions in lamproites and kimberlites based on the study of inclusions in olivine. In: Ross, J., et al. (Ed.), Kimberlites and Related Rocks: Their Composition, Occurrence, Origin and Emplacement. Blackwell Scientific Publications, Sydney, pp. 220–241.

Tomlinson, E., Jones, A., Milledge, J., 2004. High-pressure experimental growth of diamond using C–K_2CO_3–KCl as an analogue for Cl-bearing carbonate fluid. Lithos 77, 287–294.

Ukhanov, A.V., Ryabchikov, I.D., Kharkiv, A.D., 1988. Lithospheric Mantle of the Yakutian Kimberlite Province. Nauka, Moscow. 250 pp.

Vasilenko, V.B., Zinchuk, N.N., Krasavchikov, V.O., Kuznetsova, L.G., Khlestov, V.V., Volkova, N.I., 2002. Diamond potential estimation based on kimberlite major element chemistry. J. Geochem. Explor. 76, 93–112.

Veksler, I.V., 2004. Liquid immiscibility and its role at the magmatic–hydrothermal transition: a summary of experimental studies. Chem. Geol. 210, 7–31.

Veksler, I.V., Nielsen, T.F.D., Sokolov, S.V., 1998. Mineralogy of crystallized melt inclusions from Gardiner and Kovdor ultramafic alkaline complexes: implications for carbonatite genesis. J. Petrol. 39, 2015–2031.

Watkinson, D.H., Chao, G.Y., 1973. Shortite in kimberlite from the Upper Canada Gold Mine, Ontario. J. Geol. 81, 229–233.

Webster, J.D., Kinzler, R.J., Mathez, E.A., 1999. Chloride and water solubility in basalt and andesite melts and implications for magmatic degassing. Geochim. Cosmochim. Acta 63, 729–738.

Weis, D., Demaiffe, D., 1985. A depleted mantle source for kimberlites from Zaire: Nd, Sr and Pb isotopic evidence. Earth Planet. Sci. Lett. 73, 269–277.

Zaitsev, A.N., Chakhmouradian, A.R., 2002. Calcite–amphibole–clinopyroxene rock from the Afrikanda Complex, Kola Peninsula, Russia: mineralogy and a possible link to carbonatites. II. Oxysalt minerals. Can. Mineral. 40, 103–120.

Zedgenizov, D.A., Kagi, H., Shatsky, V.S., Sobolev, N.V., 2004. Carbonatitic melts in cuboid diamonds from Udachnaya kimberlite pipe (Yakutia): evidence from vibrational spectroscopy. Mineral. Mag. 68, 61–73.

Zinchuk, N.N., Spetsius, Z.V., Zuenko, V.V., Zuev, V.M., 1993. Udachnaya Kimberlite Pipe. University of Novosibirsk, Russia. 146 pp.

Zolensky, M.E., Bodnar, R.J., Gibson, E.K., Nyquist, L.E., Reese, Y., Shih, C.Y., Wiesmann, H., 1999. Asteroidal water within fluid inclusion-bearing halite in an H5 chondrite, Monahans (1998). Science 285, 1377–1379.